

Reconciling M/L Ratios Across Cosmic Time: a Concordance IMF for Massive Galaxies

PIETER VAN DOKKUM¹ AND CHARLIE CONROY²

¹*Astronomy Department, Yale University, 219 Prospect St, New Haven, CT 06511, USA*

²*Harvard-Smithsonian Center for Astrophysics, 60 Garden Street, Cambridge, MA, USA*

ABSTRACT

The stellar initial mass function (IMF) is thought to be bottom-heavy in the cores of the most massive galaxies, with an excess of low mass stars compared to the Milky Way. However, studies of the kinematics of quiescent galaxies at $2 < z < 5$ find M/L ratios that indicate lighter IMFs. Light IMFs have also been proposed for the unexpected populations of luminous galaxies that JWST has uncovered at $z > 7$, to reduce tensions with galaxy formation models. Here we explore ‘ski slope’ IMFs that are simultaneously bottom-heavy, with a steep slope at low stellar masses, and top-heavy, with a shallow slope at high masses. We derive a form of the IMF for massive galaxies that is consistent with measurements in the local universe and yet produces relatively low M/L ratios at high redshift. This concordance IMF has slopes $\gamma_1 = 2.40 \pm 0.09$, $\gamma_2 = 2.00 \pm 0.14$, and $\gamma_3 = 1.85 \pm 0.11$ in the regimes $0.08 M_\odot - 0.5 M_\odot$, $0.5 M_\odot - 1 M_\odot$, and $> 1 M_\odot$ respectively. The IMF parameter α , the mass excess compared to a Milky Way IMF, ranges from $\log(\alpha) \approx +0.3$ for present-day galaxies to $\log(\alpha) \approx -0.1$ for their star forming progenitors. The concordance IMF applies only to the central regions of the most massive galaxies, with velocity dispersions $\sigma \sim 300 \text{ km s}^{-1}$, and their progenitors. However, it can be generalized using a previously-measured relation between α and σ . We arrive at the following modification to the Kroupa (2001) IMF for galaxies with $\sigma \gtrsim 160 \text{ km s}^{-1}$: $\gamma_1 \approx 1.3 + 4.3 \log \sigma_{160}$; $\gamma_2 \approx 2.3 - 1.2 \log \sigma_{160}$; and $\gamma_3 \approx 2.3 - 1.7 \log \sigma_{160}$, with $\sigma_{160} = \sigma / 160 \text{ km s}^{-1}$. If galaxies grow primarily inside-out, so that velocity dispersions are relatively stable, these relations should also hold at high redshift.

1. INTRODUCTION

The form of the stellar initial mass function (IMF), and its potential variation with star forming conditions, is a topic of ongoing debate (see the reviews by Bastian et al. 2010; Offner et al. 2014; Smith 2020). The question has taken on a new significance since the launch of JWST, as unexpected populations of bright and seemingly massive galaxies have been discovered at $z > 7$ (e.g., Naidu et al. 2022; Labbé et al. 2023; Xiao et al. 2023). The formation of the stellar component of these galaxies requires extremely rapid conversion of gas into stars, perhaps more rapid than can be accommodated in standard galaxy formation models (see Boylan-Kolchin 2023; Dekel et al. 2023). There is a straightforward way to reduce or even eliminate this tension, as the total mass of a stellar population is dominated by stars that have low masses and contribute very little to the light. Therefore, as pointed out by Steinhardt et al. (2023) and others (Woodrum et al. 2023; Wang et al. 2024a), if the IMF in these galaxies were top-heavy (or bottom-light) their derived masses would be lowered considerably. Galaxy formation models with top-heavy IMFs also provide better fits to the UV luminosity function at these redshifts (Inayoshi et al. 2022; Harikane et al. 2023; Yung et al. 2024; Schaerer et al. 2024).

There is good evidence that such IMFs can occur in certain environments; star clusters in the central $\sim 300 \text{ pc}$ of the Milky Way appear to have an excess of high mass stars compared to young clusters elsewhere in the disk (Lu et al. 2013; Hosek et al. 2019; Chabrier & Dumond 2024), as does the 30 Doradus cluster in the Large Magellanic Cloud (Schneider et al. 2018). Top-heavy IMFs for early galaxies have also been proposed on theoretical grounds, as higher CMB temperatures can lead to an increase in the turnover mass (Larson 1998; Bate 2023). However, the IMF in the central regions of massive early-type galaxies appears to be *bottom*-heavy, with an excess of low mass stars compared to the Milky Way (see Smith 2020, for a review). The evidence for bottom-heavy IMFs comes primarily from studies of gravity-sensitive stellar absorption lines (Cenarro et al. 2003; van Dokkum & Conroy 2010; Spiniello et al. 2012; Conroy & van Dokkum 2012b; La Barbera et al. 2013; Martín-Navarro et al. 2015; La Barbera et al. 2019), which detect the low mass stars directly, and also from higher-than-expected stellar M/L ratios derived from gravitational lensing (Treu et al. 2010; Posacki et al. 2015) and galaxy dynamics (Cappellari et al. 2012; Li et al. 2017; Shetty et al. 2020). As the old and dense central regions of massive galaxies in the present-day Universe are the likely descendants of the most luminous $z > 7$ galaxies, these results suggest that – if anything – the masses of

the JWST-discovered galaxies might be *underestimated*, by factors of 1.5–3.

In this context, massive quiescent galaxies at $z \approx 2-5$ are an important bridge population. As they lack dust and young stars their stellar masses are usually well-constrained (for an assumed IMF), and dynamical masses can be determined from their sizes and absorption line kinematics. The ratio of dynamical mass to stellar mass then constrains the form of the IMF, particularly if this ratio is close to unity: a high ratio could be attributed to some combination of dark matter, gas, and extra stellar mass, but a low ratio is only consistent with relatively light IMFs. While one study reported evidence for increased M_{dyn}/M_* ratios at $z \sim 2$ (Belli et al. 2017), most find the opposite effect, that is, a decrease compared to local values (van de Sande et al. 2013; Mendel et al. 2020; Kriek et al. 2024). As discussed in Kriek et al. (2024), the M/L ratios of quiescent galaxies at $z \sim 2$ appear to be in tension with the bottom-heavy IMFs that have been found for similar-mass galaxies at $z = 0$, when systematic effects are accounted for. Dynamical mass measurements at $z > 2$ currently have large uncertainties, but they appear to be consistent with this trend: Esdaile et al. (2021) and Carnall et al. (2024) find $M_{\text{dyn}}/M_* \sim 1$ for small samples of massive quiescent galaxies at $3 < z < 5$, when assuming a standard Kroupa or Chabrier IMF. Taken together, these results suggest a possible gradual evolution, with the youngest (generally highest redshift) massive quiescent galaxies having stellar M/L ratios consistent with a standard IMF, and the oldest (lowest redshift) galaxies having M/L ratios that indicate extra mass.

One way to reconcile these seemingly contradictory results is to appeal to complex formation histories: it may be that the stars we see in massive galaxies at $z \sim 2$ and above are only a small fraction of those in the cores of present-day ellipticals. In that case the IMF at high redshift could be quite different from the one that produced most of the stars that we see today. Massive galaxies certainly grow substantially in size and mass throughout their history, through a combination of star formation and mergers (see, e.g., Dekel et al. 2009). However, the already-high central densities of early massive galaxies (even out to $z > 7$; see Bezanson et al. 2009; Baggen et al. 2023), as well as the old ages of the cores of ellipticals (e.g., Greene et al. 2015), both strongly suggest that most of this activity happened outside of the central regions. One viable form of complex evolution that should be mentioned is a mode of late central star formation that only produces low mass stars, as has been hypothesized to occur in cooling flows (see Fabian et al. 2024).

In this paper we take a different approach. We assume that the most massive galaxies at high redshift are representative of the progenitors of the central regions of the most massive galaxies at lower redshifts, and that the behavior of the M/L ratios reflects a particular form of the IMF. We use the ob-

served M/L ratios (of living stars and remnants, and of living stars only) to constrain this form. This approach has its roots in the work of Tinsley (1980), who first pointed out that the form of the IMF near the turnoff mass could be determined from the luminosity evolution of galaxies.

2. METHODOLOGY

We systematically explore a family of IMF shapes, and ask what particular form in that family produces the lowest M/L ratios at high redshift while being consistent with the bottom-heavy IMFs that have been derived for the cores of local ellipticals.

2.1. General Functional Form

The IMFs are parameterized by the three power law segments that are familiar from the Kroupa (2001) IMF: $0.08 M_{\odot} < m < 0.5 M_{\odot}$, $0.5 M_{\odot} < m < 1 M_{\odot}$, and $m > 1 M_{\odot}$. The power law slopes in these regions are denoted with γ_1 , γ_2 , and γ_3 respectively. The Kroupa (2001) IMF, appropriate for star formation in the Milky Way disk, has $\gamma_1 = 1.3$, $\gamma_2 = 2.3$, and $\gamma_3 = 2.3$. It is shown in Fig. 1, along with the (functionally nearly identical) Chabrier (2003) IMF and the Salpeter (1955) IMF (which has $\gamma_1 = \gamma_2 = \gamma_3 = 2.35$). We use integration limits of $0.08 M_{\odot} - 100 M_{\odot}$.

Within this general framework, the family of IMFs that we explore have the following characteristics:

1. A steep slope at low masses, $2.3 \leq \gamma_1 \leq 2.7$. This is needed to reproduce the spectroscopic evidence for low mass stars reported by Conroy & van Dokkum (2012b) and many others. The upper end of the range reflects the most bottom-heavy IMF that has been found so far, in the heart of the giant elliptical galaxy NGC 1407: using a non-parametric form of the IMF, Conroy et al. (2017) find a slope of 2.7 all the way to the hydrogen burning limit. Such a steep slope has also been derived theoretically for progenitors of massive ellipticals (Chabrier et al. 2014).
2. A shallower slope at intermediate masses, that is at most as steep as the Salpeter value: $\gamma_2 \leq \gamma_1$ and $\gamma_2 \leq 2.3$. Whereas γ_1 controls the amount of mass in (living) stars, γ_2 controls the luminosity: $\sim 95\%$ of the luminosity of an old stellar population comes from stars in the range $0.5 M_{\odot} < m < 1 M_{\odot}$ (see, e.g., Fig. 2 in Conroy & van Dokkum 2012a). We also impose the criterion $\gamma_1 - \gamma_2 \leq 1.0$; as we will see later, no viable solutions come near this limit.
3. An even shallower slope at high masses, again at most as steep as Salpeter: $\gamma_3 \leq \gamma_2$ and $\gamma_3 \leq 2.3$. We also require $\gamma_2 - \gamma_3 \leq 1.0$. The high mass slope has no impact on the luminosity of the cores of ellipticals, as there

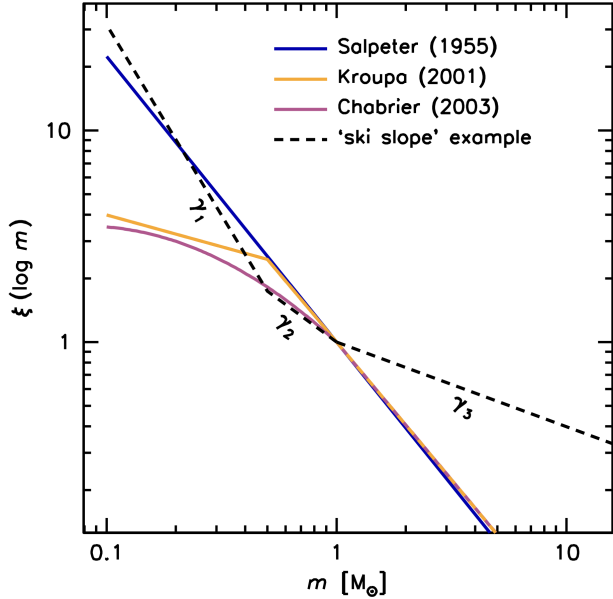


Figure 1. Illustration of the general form of the IMFs that are explored in this paper: a steep, Salpeter-like slope at low masses, followed by a flattening between $0.5 M_{\odot}$ and $1 M_{\odot}$, and a further flattening at $> 1 M_{\odot}$. This gradual flattening somewhat resembles a ski slope. For context and reference, the widely used Salpeter (1955), Kroupa (2001), and Chabrier (2003) forms are also shown. Ski slope IMFs are simultaneously bottom-heavy and top-heavy compared to the IMF of the Milky Way.

are no living stars with $m > 1 M_{\odot}$. Instead, it controls the luminosity of the stellar population at younger ages and higher redshifts (together with γ_2), and the amount of mass at late times that is locked up in remnants (neutron stars and black holes). Remnants are a small fraction of the total mass for a Salpeter IMF, but they become increasingly important for more bottom-light and/or top-heavy IMFs. As noted by Maraston (1998) and others, the total mass of a stellar population with a top-heavy IMF is often remnant-dominated at late times.

The general shape of the IMFs that we explore is illustrated with the broken line in Fig. 1. The limiting case is a near-Salpeter IMF, with $\gamma_1 = \gamma_2 = \gamma_3 = 2.3$, but the general form is *both* bottom-heavy and top-heavy.

2.2. Observational Constraints

We focus on three key aspects when assessing the viability of a particular IMF: the number of low mass stars for old ages, which has to match the constraints from absorption line studies; the total M/L ratio for old ages, which has to match constraints from lensing and dynamics; and the total M/L ratio for young ages, which should be as low as possible while still satisfying the first two constraints.

For convenience, and to allow straightforward comparisons to the literature, the diagnostic parameters are expressed in terms of the mass excess compared to the standard Kroupa (2001) IMF:

$$\alpha \equiv \frac{(M/L)[\gamma_1, \gamma_2, \gamma_3]}{(M/L)[1.3, 2.3, 2.3]}. \quad (1)$$

Luminosities are calculated in the SDSS r band. Masses can refer to the total stellar mass, that is, living stars and remnants (α_{tot}), or to the mass in living stars only (α_{liv}). As $\sim 70\%$ of the total living mass is locked up in stars with masses $< 0.5 M_{\odot}$, α_{liv} is a proxy for the ratio of the number of low mass stars to the number of turnoff stars.

With these definitions in place, we impose the following quantitative requirements on viable IMFs:

$$\alpha_{\text{liv}} > 1.6 \quad (\text{age} = 12.5 \text{ Gyr}) \quad (2)$$

$$\alpha_{\text{tot}} < 2.3 \quad (\text{age} = 12.5 \text{ Gyr}) \quad (3)$$

$$\alpha_{\text{tot}} < 1.3 \quad (\text{age} = 0.5 \text{ Gyr}) \quad (4)$$

The first constraint ensures that there is an excess of low mass stars compared to the Milky Way IMF. It is based on the spectral analysis of Conroy & van Dokkum (2012b), who find $1.6 \lesssim \alpha_{\text{tot}} \lesssim 2.0$ for the most massive and Mg-enhanced galaxies. Note that Conroy & van Dokkum (2012b) express their results in terms of α_{tot} rather than α_{liv} . For $\gamma_3 = 2.3$, as is assumed in that study, $\alpha_{\text{liv}} \approx 1.1\alpha_{\text{tot}}$. The second constraint is to ensure that the total mass does not exceed constraints from lensing and dynamics. Posacki et al. (2015) find $\alpha_{\text{tot}} \approx 1.6$ for a sample of strong lenses with $\sigma \sim 300 \text{ km s}^{-1}$, and Mendel et al. (2020) find $\alpha_{\text{tot}} \approx 2.2$ for SDSS galaxies in the same mass range. A limit is needed: as we show later, IMFs with shallow high mass slopes (i.e., low γ_3) are often remnant-dominated, yielding very high values of α_{tot} .

The third constraint is of a different nature than the other two. As explained in the Introduction, our aim is to determine whether it is possible to have low values of α at high redshift while satisfying the observational constraints at low redshift. The constraint $\alpha_{\text{tot}} < 1.3$ for young ages simply selects the IMFs that produce the lowest M/L ratios in this family of IMFs.

2.3. Grid Search

We perform a straightforward grid search to determine which IMFs satisfy the observational constraints. The grid consists of all IMFs that satisfy the constraints on γ_1 , γ_2 , and γ_3 that were laid out in § 2.1, with steps of 0.1 in each of the three parameters. Masses and luminosities are determined with the Python implementation¹ of the flexible stellar

¹ Python-FSPS, <https://dfm.io/python-fsps/current/>

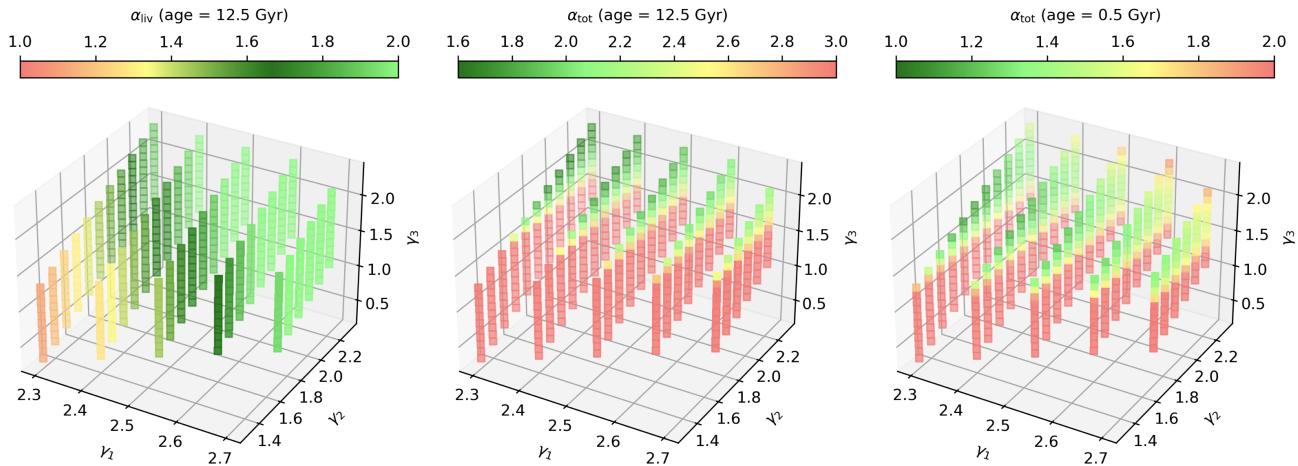


Figure 2. Values of the IMF parameter α for all 484 ‘ski slope’ IMFs that are considered in this study, as a function of the three power law slopes γ_1 , γ_2 , γ_3 that define the shape. In each panel the color palette is such that red is disfavored/disallowed and green is favored/allowed. *Left:* α_{liv} , the mass excess in living stars, for an age of 12.5 Gyr. Many IMFs satisfy the constraint $\alpha_{\text{liv}} > 1.6$. *Middle:* α_{tot} , the total mass excess, for an age of 12.5 Gyr. This is a strong function of the high mass slope, γ_3 . Shallow high mass slopes produce too many remnants, and are disallowed by the criterion $\alpha_{\text{tot}} < 2.3$. *Right:* α_{tot} for an age of 0.5 Gyr. The lowest values of α_{tot} are in the range 1.1–1.3.

population synthesis (FSPS) suite (Conroy et al. 2009; Conroy & Gunn 2010), for dust-free single stellar populations with solar metallicity. The default MIST isochrones (Choi et al. 2016) and MILES spectral library (Falcón-Barroso et al. 2011) are used.

For each stellar population we determine the mass in living stars, the total mass (in living stars and stellar remnants), and the luminosity in the SDSS r band, for an age of 0.5 Gyr and an age of 12.5 Gyr. The young age corresponds to the approximate luminosity-weighted ages of the $3 < z < 5$ galaxies in Esdaile et al. (2021) and Carnall et al. (2024). An age of 12.5 Gyr is appropriate for the cores of massive galaxies (see, e.g., van Dokkum et al. 2017), and also consistent with the age of the $z \sim 4$ galaxies if they evolve passively to the present. With the masses and luminosities for each IMF at both ages, as well as the equivalent values for a standard Kroupa (2001) IMF, the diagnostics α_{liv} , α_{tot} (at 12.5 Gyr) and α_{tot} (at 0.5 Gyr) are calculated.

3. RESULTS

3.1. Allowed IMF Shapes

The results for all 484 IMFs are visualized in Fig. 2. The left and middle panels show α_{liv} and α_{tot} , respectively, for an age of 12.5 Gyr. The right panel shows α_{tot} for 0.5 Gyr. In each panel the color coding is chosen such that green indicates ‘allowed’ (or ‘preferred’), and red indicates ‘not allowed’.

Turning first to the results for α_{liv} at 12.5 Gyr (left panel), we find that the constraint $\alpha_{\text{liv}} > 1.6$ is satisfied for a wide range of IMF shapes. That is, most of the IMFs in this family have a relatively high number of low mass stars. This is a direct consequence of the chosen range of γ_1 , between Salpeter

(2.3) and steeper than Salpeter (2.7). At fixed α_{liv} there is an interplay between γ_1 and γ_2 , such that the ratio of the number of low mass stars to the number of turnoff stars is conserved. Specifically, for $1.7 < \alpha_{\text{liv}} < 1.9$ we find $\gamma_2 \approx 5.9 - 1.6 \times \gamma_1$. Note that the results for α_{liv} are entirely independent of γ_3 , the slope of the IMF beyond the turnoff mass.

Turning to the results for α_{tot} at 12.5 Gyr, we find that for most of the IMFs the value of α_{tot} is too high: the constraint $\alpha_{\text{tot}} < 2.3$ is satisfied only in a small region of parameter space. The key parameter is γ_3 ; shallow high mass slopes produce too many stellar remnants, leading to M/L ratios that are higher than is allowed by lensing and dynamical measurements of massive $z = 0$ galaxies. To illustrate the strong dependence on γ_3 , all IMFs with $\gamma_3 < 1.5$ have $\alpha_{\text{tot}} > 3$, and all IMFs with $\gamma_3 > 2$ have $\alpha_{\text{tot}} < 2.3$.

The right panel of Fig. 2 shows α_{tot} for young ages. The results are superficially similar to the 12.5 Gyr panel, but the scale is different: whereas the lowest value of α_{tot} at 12.5 Gyr is 1.62, it is only 1.13 at 0.5 Gyr – that is, very close to a standard Chabrier or Kroupa IMF. Importantly, the green region of parameter space, indicating the lowest values of α_{tot} , has considerable overlap with the green regions in the other two panels. This means that there are viable IMF solutions that satisfy all the constraints of § 2.2.

3.2. Concordance IMF

Applying the criteria of Eqs. 2, 3, and 4 yields 20 viable IMFs that are all very similar. The mean power law slopes are

$$\gamma_1 = 2.40 \pm 0.09;$$

$$\gamma_2 = 2.00 \pm 0.14;$$

$$\gamma_3 = 1.85 \pm 0.11,$$

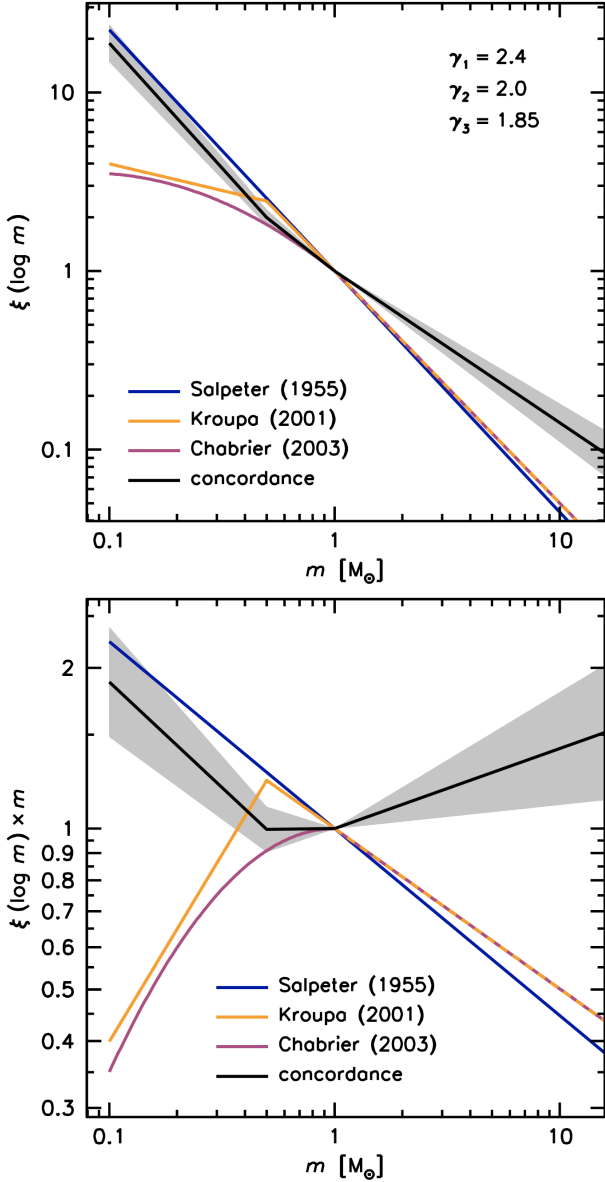


Figure 3. The ‘concordance’ IMF that we propose here for massive galaxies, compared to standard forms. The same information is shown in the top and bottom panels, but in the bottom panel the y-axis is multiplied by m to reduce the dynamic range and bring out the differences between the IMFs. The turnover at $1 M_{\odot}$ is not significant; IMFs with $\gamma_1 = 2.4$ and $\gamma_2 = \gamma_3 = 1.9$ produce very similar results.

where the uncertainty is taken to be the rms range among the 20 IMFs. This concordance IMF is shown in Fig. 3. It is similar to the Salpeter IMF in terms of its ratio of low mass stars to turnoff stars, but flatter at high masses. The key turnover is at $0.5 M_{\odot}$: the slope changes at this point in all 20 viable IMFs, by 0.4 ± 0.2 . The turnover at $1 M_{\odot}$ is not significant; of the 20 viable models, 7 have $\gamma_2 = \gamma_3$.

The IMF is remarkably well constrained, both at the low mass end and at the high mass end. As explained above, the three limits of Eqs. 2, 3, and 4 all control different aspects of the IMF. The low mass slope is tightly constrained by the observed mass excess in low mass stars. The high mass slope is constrained by two competing effects: if it were shallower, stellar remnants would violate lensing and dynamical constraints for old ages, and if it were steeper, the M/L ratios for young ages would be too high.

3.3. M/L Ratios Over Cosmic Time

Returning to the questions that were asked in the Introduction, we now consider how the IMF parameter α (the mass excess compared to a Kroupa IMF) changes with redshift. The time evolution of the M/L_r ratio is shown in the left panel of Fig. 4, for both the concordance IMF and a standard Kroupa IMF. In the right panel we show the time evolution of α , the ratio of these two curves. The IMF parameter monotonically increases with age, going from $\lesssim -0.1$ at ages of $\lesssim 50$ Myr to $\approx +0.3$ at 12.5 Gyr.

Turning to the galaxy populations that were discussed in the Introduction, the concordance IMF reproduces the large mass excess, and the large number of low mass stars, observed in the cores of present-day massive elliptical galaxies; reproduces the smaller excess of 0–0.2 dex that has been found for young quiescent galaxies at $z = 2-5$; and produces a mass deficit for massive star forming $z > 7$ galaxies, in better agreement with galaxy formation models.

3.4. Dependence on the Low Mass Cutoff

In our analysis the lower integration limit of the IMF is the hydrogen burning limit of $0.08 M_{\odot}$ (Chabrier et al. 2023), that is, it is assumed that the mass locked up in brown dwarfs is negligible. For a Milky Way IMF the precise lower limit is not important as most of the stellar mass is in stars near the turnover; for a Kroupa IMF, changing the lower limit to $0.03 M_{\odot}$ increases the total mass by 2% and changing it to $0.01 M_{\odot}$ increases the mass by 3%. However, for a Salpeter IMF the total mass is very sensitive to the low mass cutoff, increasing by a factor of 1.4 going from $0.08 M_{\odot}$ to $0.03 M_{\odot}$. For a lower limit of $0.01 M_{\odot}$ the increase is a factor of 2.2, which means that most of the stellar mass is in the form of brown dwarfs.

As ski slope IMFs have a Salpeter-like low mass slope, their total mass is also very sensitive to the low mass cutoff. We repeated the analysis for integration limits of $0.03 M_{\odot}$ and $0.01 M_{\odot}$, and find that *no* IMFs satisfy the criteria of § 2.2. Relaxing the criteria to $\alpha_{\text{tot}} < 2.5$ (age = 12.5 Gyr) and $\alpha_{\text{tot}} < 1.5$ (age = 0.5 Gyr), there is one solution for a cutoff of $0.03 M_{\odot}$, with $\gamma_1 = 2.3$, $\gamma_2 = 2.1$, and $\gamma_3 = 1.8$, and still no solution for a cutoff of $0.01 M_{\odot}$.

We infer that a turnover near the hydrogen burning limit is required in the context of ski slope IMFs, as otherwise the to-

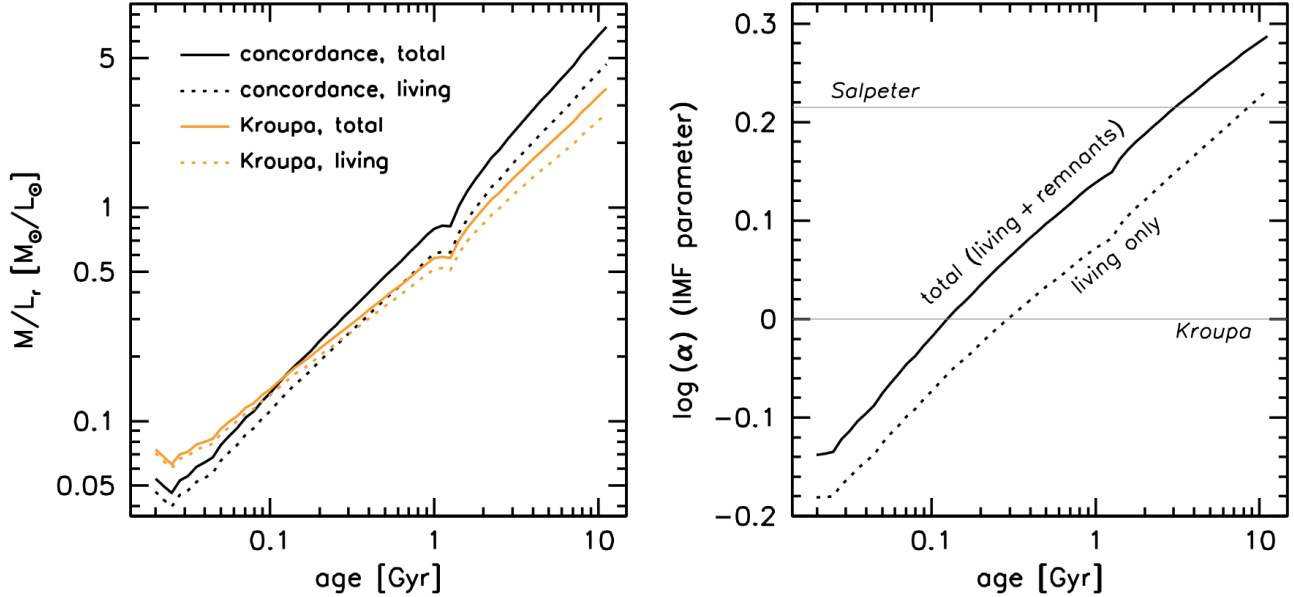


Figure 4. *Left panel:* Relation between M/L_r ratio and age, for the concordance IMF and for a standard Kroupa (2001) IMF. For old ages the concordance M/L ratios are higher than the Kroupa M/L ratios, but this reverses for the youngest ages. *Right panel:* IMF parameter α as a function of age, for the concordance IMF. This relation is the logarithmic offset between the two curves in the left panel. While the mass excess is larger than that of a Salpeter IMF for old ages, it is close to a Kroupa or Chabrier IMF for ages of 0.1–0.5 Gyr. For the youngest ages there is a mass deficit with respect to the Kroupa IMF.

tal M/L ratios would exceed constraints from dynamics and lensing. The steep slope at low masses and the sharp cutoff at $0.08 M_\odot$ should be viewed as a simplified parameterization of a shift in the turnover mass from $\sim 0.3 M_\odot$ for the Milky Way to $\sim 0.1 M_\odot$ for the concordance IMF. The actual form of the low mass IMF may be similar to the IMFs explored in Chabrier et al. (2014), which combine slopes of 2.3–2.7 with a turnover near $0.1 M_\odot$.

3.5. Dependence on Velocity Dispersion

So far the focus has been on a single form of the IMF, but the IMF parameter α correlates with mass, velocity dispersion, metallicity, and (within a galaxy) radius (see, e.g., Conroy & van Dokkum 2012b; Martín-Navarro et al. 2015; Mendel et al. 2020). Our analysis can be extended by taking this variation into account, thereby enabling a compact parameterization of the full range of IMF shapes from Milky Way-like galaxies to the cores of massive ellipticals.

We can take a first step toward such a description by assuming that the form of the IMF varies smoothly as a function of velocity dispersion. Defining $\sigma_x \equiv \sigma/x \text{ km s}^{-1}$, a bisector fit to the Conroy & van Dokkum (2012b) data gives

$$\log \alpha_{\text{tot}} \approx 0.22 + 1.16 \log \sigma_{250}, \quad (5)$$

for $\sigma \gtrsim 160 \text{ km s}^{-1}$. The concordance IMF has $\alpha_{\text{tot}} = 1.95$ for an age of 12.5 Gyr, and is therefore appropriate for galaxies with $\sigma \approx 290 \text{ km s}^{-1}$. Using Eq. 5, and assuming that galaxies with $\sigma \lesssim 160 \text{ km s}^{-1}$ have a standard Kroupa (2001) IMF, we

obtain the following relations between the power law slopes of the IMF and the velocity dispersion:

$$\begin{aligned} \gamma_1 &\approx 1.3 + 4.3 \log \sigma_{160}; \\ \gamma_2 &\approx 2.3 - 1.2 \log \sigma_{160}; \\ \gamma_3 &\approx 2.3 - 1.7 \log \sigma_{160}, \end{aligned} \quad (6)$$

for $\sigma \gtrsim 160 \text{ km s}^{-1}$. For lower velocity dispersions we simply have $\gamma_1 = 1.3$, $\gamma_2 = \gamma_3 = 2.3$. The IMF parameter α of this generalized concordance IMF is shown in Fig. 5.

For reference, measurements from Conroy & van Dokkum (2012b) are overplotted as light red dots. These data are well described by the 12.5 Gyr old model, as expected. The other lines are the implied relations for younger ages. If galaxies primarily grow inside-out their velocity dispersions do not change very much with time. This means that these same relations can also be used at high redshift, as long as σ can be measured, either directly from spectra or estimated from sizes and masses (e.g., Bezanson et al. 2011).

4. DISCUSSION

Our analysis shows that it is possible, with a single form of the IMF, to have M/L ratios that are $\lesssim 0.8\times$ that of a Milky Way IMF at young ages and $\approx 2\times$ that of a Milky Way IMF at old ages. The proposed concordance IMF with $\gamma_1 = 2.4$, $\gamma_2 = 2.0$, and $\gamma_3 = 1.85$ ties together observations of the cores of massive galaxies at $z = 0$, dynamical studies of quiescent galaxies at $2 < z < 5$, and recent JWST observations of unexpectedly dense and massive galaxies at $z > 7$. At the highest

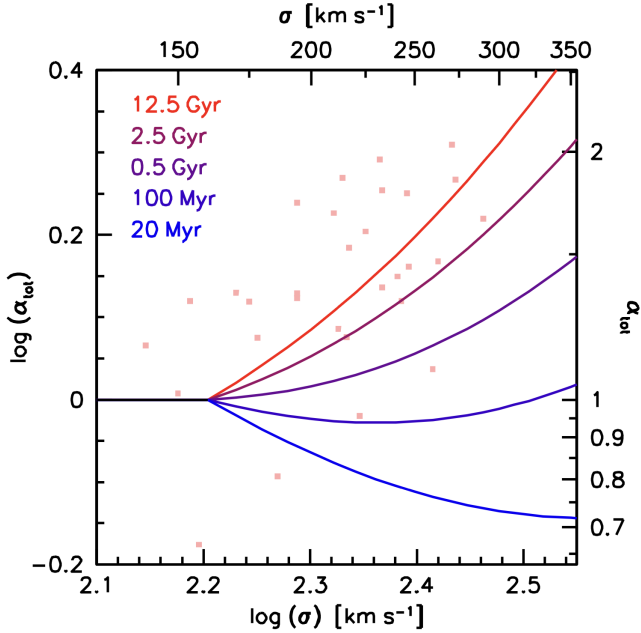


Figure 5. Relation between the IMF parameter α and velocity dispersion, for the generalized concordance IMF of Eq. 6. Data for the central regions of nearby early-type galaxies from Conroy & van Dokkum (2012b) are shown in light red. By construction, the model for an age of 12.5 Gyr fits these data well. The other lines show the behavior at younger ages.

redshifts the mass-increasing effect of a steep low mass slope is more than compensated by the luminosity-increasing effect of a flat high mass slope. The concordance IMF, and the generalized form (Eq. 6), can be implemented in a straightforward way, as γ_1 , γ_2 , and γ_3 are defined over the same mass intervals as the Kroupa (2001) IMF (which has $\gamma_1 = 1.3$, and $\gamma_2 = \gamma_3 = 2.3$).

We note that our results are insensitive to progenitor bias, that is, the fact that samples of massive galaxies at high redshift always represent only a subset of all progenitors of such galaxies today (Franx & van Dokkum 1996; van Dokkum & Franx 2001; Leja et al. 2013; Torrey et al. 2017). The concordance IMF produces a straightforward age dependence of the IMF parameter α , irrespective of the redshift, history, or future of a particular galaxy. In this context it is encouraging that the concordance IMF reproduces the low M_{dyn}/M_* ratios, consistent with $\log \alpha \lesssim 0$, that have been reported for massive, compact star forming galaxies at $z = 2-3$ (Barro et al. 2014, 2017; van Dokkum et al. 2015).

Compared to standard Kroupa and Chabrier IMFs, the changes are modest for the youngest ages — for an age of 100 Myr we have $\log \alpha \approx 0$, independent of velocity dispersion — and a conclusion from this study is that a Milky Way-like IMF produces reasonable masses for massive JWST-discovered galaxies. The effects can be more complex than is indicated in Figs. 4 and 5, however, as changing the IMF not

only changes the luminosities but also the colors. To assess the magnitude of this effect the three Balmer break galaxies at $z = 7-8$ of Wang et al. (2024b) were re-fit with the concordance IMF, a standard Kroupa IMF, and a Chabrier IMF. The differences in $\log M_*$ between the concordance IMF and the standard IMFs are in the range -0.3 to -0.2 , broadly consistent with expectations (B. Wang, priv. comm.).

We are not the first to explain observations of massive early-type galaxies with IMFs that are simultaneously bottom-heavy and top-heavy, although the precise slopes and mass ranges vary. Arrigoni et al. (2010) find that a mildly flat slope at $> 1 M_\odot$, with $\gamma_3 \approx 2.15$, can explain the slope of the $[\text{Mg}/\text{Fe}] - \sigma$ relation for early-type galaxies. In the same vein, den Brok et al. (2024) find a steep low mass slope and a flat high mass slope from a combined analysis of gravity-sensitive spectral features and stellar abundances. van de Sande et al. (2015) introduce an IMF with a slope of ≈ 1.4 in the mass range $1-4 M_\odot$ (and 2.3 at lower masses) to explain the relation between color and M/L ratio for a sample of massive quiescent galaxies out to $z \sim 2$. Peacock et al. (2017) and Coulter et al. (2017) favor these kinds of IMFs to account for the relatively large numbers of X-ray binaries (i.e., stellar remnants) in elliptical galaxies, while maintaining a steep low mass slope. Specifically, the Coulter et al. (2017) form has a slope of 3.8 at $< 0.5 M_\odot$ and a slope of 2.0 for all masses $> 0.5 M_\odot$. In summary, mildly flatter slopes beyond $1 M_\odot$ are not only allowed by previous work but appear to be favored, for a variety of reasons.

Our results can be tested in various ways. Thanks to JWST the number of high redshift quiescent galaxies with dynamical masses is expected to increase rapidly in the coming years, and it will be interesting to see if M_{dyn}/M_* ratios show a similar trend as α does in Fig. 4. Care must be taken, as many high redshift galaxies are likely supported by rotation, complicating the interpretation of observed velocity dispersions (see, e.g., van der Wel et al. 2011; Newman et al. 2018; Bezanson et al. 2018). Special objects, such as the Einstein ring JWST-ER1 (van Dokkum et al. 2024; Mercier et al. 2024), provide unique information that can be used to calibrate larger samples.² Direct measurements of low mass stars at significant redshifts would be even more constraining: as shown by the dotted line in Fig. 4, the mass excess in living stars should show a similar trend as the total mass excess, and the interpretation of the data is more straightforward (as it is independent of the mass in stellar remnants, dark matter, and gas).³ Stellar population fits with

² The reported values of $\log(\alpha)$ currently range between 0 and 0.3 for this object, depending on the assumed redshift of the ring. A Cycle 3 JWST program (GO-5883; PI R. Gavazzi) will resolve this question.

³ The Cycle 3 JWST program GO-5629 (PI: M. Kriek) aims to perform this measurement at $z \sim 0.7$.

non-parametric forms of the IMF may be able to differentiate between a constant steep slope below $1 M_{\odot}$ and a gradually increasing one. Encouragingly, there is evidence for such an increasing slope in NGC 1407, the only galaxy that has been analyzed this way so far (Conroy et al. 2017). Lastly, an important caveat is that the steep low mass slope is currently based on a single methodology, the measurement of gravity-sensitive absorption lines in the integrated spectra of early-type galaxies. All other observations could also be explained by a more straightforward top-heavy, or bottom-light, IMF, as stellar remnants would take the place of low mass stars in producing the high M/L ratios of present-day massive galaxies. Independent tests of the low mass IMF, such as the one we introduced in van Dokkum & Conroy (2021), would be highly valuable.⁴

The physical origin of IMFs that are simultaneously bottom-heavy and top-heavy is unclear. The behavior of the IMF at low masses has long been linked to the Jeans mass and its dependence on temperature, density, and Mach number. In extreme environments the low-mass IMF can be suppressed due to the $T^{3/2}$ temperature dependence of the Jeans mass (Larson 1998; Krumholz 2006; Bate 2009, 2023), or enhanced if the $\rho^{-1/2}$ density dependence or Mach number dependence dominates (e.g., Hopkins 2013; Chabrier et al. 2014; Tanvir et al. 2022; Tanvir & Krumholz 2024), but it is difficult to do both at the same time (see, e.g., Bate 2023). A different process may operate at high masses. Models based on Press-Schechter-like arguments applied to turbulent molecular clouds (Hennebelle & Chabrier 2008; Hopkins 2013; Chabrier et al. 2014) directly link the high-mass IMF slope to the spectral index of the turbulent velocity power spectrum, with steeper spectra giving rise to shallower high-mass IMF slopes. These models have been tested and refined with hydrodynamical simulations (Nam et al. 2021), although it remains to be seen whether the required modifications to the spectral index occur in realistic environments. To summarize, γ_1 may be largely determined by the Jeans mass and γ_3 by the index of the turbulent power spectrum, but more work is needed to test this.

It may also be that the observed IMF is a combination of star formation in different local environments within early galaxies, with the densest regions producing the steep low mass slope and the regions that are most exposed to radiation producing the flat high mass slope. *JWST* results have

shown that many early galaxies have extremely high central surface densities (Baggen et al. 2023; Carnall et al. 2024), lending some observational support to this idea. Such hybrid IMFs have been developed previously in the framework of the ‘integrated galactic IMF’ (IGIMF; Kroupa & Weidner 2003), and the IMF that Jeřábková et al. (2018), Yan et al. (2019, 2021), and Haslbauer et al. (2024) propose for high metallicity, high star formation rate environments is qualitatively quite similar to the concordance IMF. Fontanot et al. (2018), working from similar concepts as Kroupa & Weidner (2003), introduce physically-motivated IMFs that have a break at $1 M_{\odot}$ with a steep slope at low masses and a shallow slope at high masses. As shown in Fontanot et al. (2023), these IMFs reproduce the M/L ratios of present-day ellipticals well, although they underpredict the number of low mass stars (the mass excess with respect to the Milky Way IMF is largely in the form of remnants, not low mass stars, in these models).

Several of the questions that are raised in the preceding paragraphs could be addressed if local analogs could be studied. Returning to the evidence for top-heavy IMFs discussed in the Introduction, the high mass slope in 30 Doradus is $1.90^{+0.37}_{-0.26}$ (Schneider et al. 2018), similar to that of the concordance IMF. It would be very interesting — although observationally challenging; see, e.g., Fahrion & De Marchi (2024) — to determine if there is an upturn at low masses in this cluster. We note that if such analogs exist in the Local Group, it would imply that the observed relations with global galaxy properties such as σ are proxies for the preponderance of particular local conditions within the galaxies.

As a final remark, we acknowledge the long history of appealing to IMF variation as a means of explaining real or imagined observational tensions, and that in such previous cases a more prosaic explanation was usually found. We therefore suggest adopting the concordance IMF with caution, for now.

We thank Mariska Kriek and Bingjie Wang for their comments on the manuscript. Bingjie Wang also fitted the galaxies in her paper with the concordance IMF. We are grateful to the referee, Mark Krumholz, for insightful comments that improved the paper. Finally, we thank the organizers of the 2011 Galaxy Formation conference in Durham, as this was when we first considered ‘ski slope’ IMFs as a potential way to reconcile seemingly contradictory results in the literature.

REFERENCES

- Arrighoni, M., Trager, S. C., Somerville, R. S., & Gibson, B. K. 2010, *MNRAS*, 402, 173,
doi: 10.1111/j.1365-2966.2009.15924.x

⁴ In yet another Cycle 3 *JWST* program, GO-4757 (PI: P. van Dokkum), we plan to use the strength of near-IR H₂O features to constrain the low mass IMF.

- Baggen, J. F. W., van Dokkum, P., Labbé, I., et al. 2023, *ApJL*, 955, L12, doi: [10.3847/2041-8213/acf5ef](https://doi.org/10.3847/2041-8213/acf5ef)
- Barro, G., Trump, J. R., Koo, D. C., et al. 2014, *ApJ*, 795, 145, doi: [10.1088/0004-637X/795/2/145](https://doi.org/10.1088/0004-637X/795/2/145)
- Barro, G., Kriek, M., Pérez-González, P. G., et al. 2017, *ApJL*, 851, L40, doi: [10.3847/2041-8213/aa9f0d](https://doi.org/10.3847/2041-8213/aa9f0d)
- Bastian, N., Covey, K. R., & Meyer, M. R. 2010, *ARA&A*, 48, 339, doi: [10.1146/annurev-astro-082708-101642](https://doi.org/10.1146/annurev-astro-082708-101642)
- Bate, M. R. 2009, *MNRAS*, 392, 1363, doi: [10.1111/j.1365-2966.2008.14165.x](https://doi.org/10.1111/j.1365-2966.2008.14165.x)
- . 2023, *MNRAS*, 519, 688, doi: [10.1093/mnras/stac3481](https://doi.org/10.1093/mnras/stac3481)
- Belli, S., Newman, A. B., & Ellis, R. S. 2017, *ApJ*, 834, 18, doi: [10.3847/1538-4357/834/1/18](https://doi.org/10.3847/1538-4357/834/1/18)
- Bezanson, R., van Dokkum, P. G., Tal, T., et al. 2009, *ApJ*, 697, 1290, doi: [10.1088/0004-637X/697/2/1290](https://doi.org/10.1088/0004-637X/697/2/1290)
- Bezanson, R., van Dokkum, P. G., Franx, M., et al. 2011, *ApJL*, 737, L31+, doi: [10.1088/2041-8205/737/2/L31](https://doi.org/10.1088/2041-8205/737/2/L31)
- Bezanson, R., van der Wel, A., Pacifici, C., et al. 2018, *ApJ*, 858, 60, doi: [10.3847/1538-4357/aabc55](https://doi.org/10.3847/1538-4357/aabc55)
- Boylan-Kolchin, M. 2023, *Nature Astronomy*, 7, 731, doi: [10.1038/s41550-023-01937-7](https://doi.org/10.1038/s41550-023-01937-7)
- Cappellari, M., McDermid, R. M., Alatalo, K., et al. 2012, *Nature*, 484, 485, doi: [10.1038/nature10972](https://doi.org/10.1038/nature10972)
- Carnall, A. C., Cullen, F., McLure, R. J., et al. 2024, arXiv e-prints, arXiv:2405.02242, doi: [10.48550/arXiv.2405.02242](https://doi.org/10.48550/arXiv.2405.02242)
- Cenarro, A. J., Gorgas, J., Vazdekis, A., Cardiel, N., & Peletier, R. F. 2003, *MNRAS*, 339, L12, doi: [10.1046/j.1365-8711.2003.06360.x](https://doi.org/10.1046/j.1365-8711.2003.06360.x)
- Chabrier, G. 2003, *PASP*, 115, 763
- Chabrier, G., Baraffe, I., Phillips, M., & Debras, F. 2023, *A&A*, 671, A119, doi: [10.1051/0004-6361/202243832](https://doi.org/10.1051/0004-6361/202243832)
- Chabrier, G., & Dumond, P. 2024, *ApJ*, 966, 48, doi: [10.3847/1538-4357/ad33c0](https://doi.org/10.3847/1538-4357/ad33c0)
- Chabrier, G., Hennebelle, P., & Charlot, S. 2014, *ApJ*, 796, 75, doi: [10.1088/0004-637X/796/2/75](https://doi.org/10.1088/0004-637X/796/2/75)
- Choi, J., Dotter, A., Conroy, C., et al. 2016, *ApJ*, 823, 102, doi: [10.3847/0004-637X/823/2/102](https://doi.org/10.3847/0004-637X/823/2/102)
- Conroy, C., & Gunn, J. E. 2010, *ApJ*, 712, 833, doi: [10.1088/0004-637X/712/2/833](https://doi.org/10.1088/0004-637X/712/2/833)
- Conroy, C., Gunn, J. E., & White, M. 2009, *ApJ*, 699, 486, doi: [10.1088/0004-637X/699/1/486](https://doi.org/10.1088/0004-637X/699/1/486)
- Conroy, C., & van Dokkum, P. 2012a, *ApJ*, 747, 69, doi: [10.1088/0004-637X/747/1/69](https://doi.org/10.1088/0004-637X/747/1/69)
- Conroy, C., & van Dokkum, P. G. 2012b, *ApJ*, 760, 71, doi: [10.1088/0004-637X/760/1/71](https://doi.org/10.1088/0004-637X/760/1/71)
- Conroy, C., van Dokkum, P. G., & Villaume, A. 2017, *ApJ*, 837, 166, doi: [10.3847/1538-4357/aa6190](https://doi.org/10.3847/1538-4357/aa6190)
- Coulter, D. A., Lehmer, B. D., Eufrasio, R. T., et al. 2017, *ApJ*, 835, 183, doi: [10.3847/1538-4357/835/2/183](https://doi.org/10.3847/1538-4357/835/2/183)
- Dekel, A., Sari, R., & Ceverino, D. 2009, *ApJ*, 703, 785, doi: [10.1088/0004-637X/703/1/785](https://doi.org/10.1088/0004-637X/703/1/785)
- Dekel, A., Sarkar, K. C., Birnboim, Y., Mandelker, N., & Li, Z. 2023, *MNRAS*, 523, 3201, doi: [10.1093/mnras/stad1557](https://doi.org/10.1093/mnras/stad1557)
- den Brok, M., Krajnović, D., Emsellem, E., et al. 2024, *MNRAS*, 530, 3278, doi: [10.1093/mnras/stae912](https://doi.org/10.1093/mnras/stae912)
- Esdaile, J., Glazebrook, K., Labbé, I., et al. 2021, *ApJL*, 908, L35, doi: [10.3847/2041-8213/abe11e](https://doi.org/10.3847/2041-8213/abe11e)
- Fabian, A. C., Sanders, J. S., Ferland, G. J., et al. 2024, *MNRAS*, 531, 267, doi: [10.1093/mnras/stae1206](https://doi.org/10.1093/mnras/stae1206)
- Fahrion, K., & De Marchi, G. 2024, *A&A*, 681, A20, doi: [10.1051/0004-6361/202348097](https://doi.org/10.1051/0004-6361/202348097)
- Falcón-Barroso, J., Sánchez-Blázquez, P., Vazdekis, A., et al. 2011, *A&A*, 532, A95, doi: [10.1051/0004-6361/201116842](https://doi.org/10.1051/0004-6361/201116842)
- Fontanot, F., La Barbera, F., De Lucia, G., Pasquali, A., & Vazdekis, A. 2018, *MNRAS*, 479, 5678, doi: [10.1093/mnras/sty1768](https://doi.org/10.1093/mnras/sty1768)
- Fontanot, F., La Barbera, F., De Lucia, G., et al. 2023, arXiv e-prints, arXiv:2311.12932, doi: [10.48550/arXiv.2311.12932](https://doi.org/10.48550/arXiv.2311.12932)
- Franx, M., & van Dokkum, P. G. 1996, in *New Light on Galaxy Evolution*, ed. R. Bender & R. L. Davies, Vol. 171, 233, doi: [10.48550/arXiv.astro-ph/9603029](https://doi.org/10.48550/arXiv.astro-ph/9603029)
- Greene, J. E., Janish, R., Ma, C.-P., et al. 2015, *ApJ*, 807, 11, doi: [10.1088/0004-637X/807/1/11](https://doi.org/10.1088/0004-637X/807/1/11)
- Harikane, Y., Ouchi, M., Oguri, M., et al. 2023, *ApJS*, 265, 5, doi: [10.3847/1538-4365/acaaa9](https://doi.org/10.3847/1538-4365/acaaa9)
- Haslbauer, M., Yan, Z., Jerabkova, T., et al. 2024, arXiv e-prints, arXiv:2405.05313, doi: [10.48550/arXiv.2405.05313](https://doi.org/10.48550/arXiv.2405.05313)
- Hennebelle, P., & Chabrier, G. 2008, *ApJ*, 684, 395, doi: [10.1086/589916](https://doi.org/10.1086/589916)
- Hopkins, P. F. 2013, *MNRAS*, 433, 170, doi: [10.1093/mnras/stt713](https://doi.org/10.1093/mnras/stt713)
- Hosek, Matthew W., J., Lu, J. R., Anderson, J., et al. 2019, *ApJ*, 870, 44, doi: [10.3847/1538-4357/aaef90](https://doi.org/10.3847/1538-4357/aaef90)
- Inayoshi, K., Harikane, Y., Inoue, A. K., Li, W., & Ho, L. C. 2022, *ApJL*, 938, L10, doi: [10.3847/2041-8213/ac9310](https://doi.org/10.3847/2041-8213/ac9310)
- Jeřábková, T., Hasani Zonoozi, A., Kroupa, P., et al. 2018, *A&A*, 620, A39, doi: [10.1051/0004-6361/201833055](https://doi.org/10.1051/0004-6361/201833055)
- Kriek, M., Beverage, A. G., Price, S. H., et al. 2024, *ApJ*, 966, 36, doi: [10.3847/1538-4357/ad2df9](https://doi.org/10.3847/1538-4357/ad2df9)
- Kroupa, P. 2001, *MNRAS*, 322, 231
- Kroupa, P., & Weidner, C. 2003, *ApJ*, 598, 1076, doi: [10.1086/379105](https://doi.org/10.1086/379105)
- Krumholz, M. R. 2006, *ApJL*, 641, L45, doi: [10.1086/503771](https://doi.org/10.1086/503771)
- La Barbera, F., Ferreras, I., Vazdekis, A., et al. 2013, *MNRAS*, 433, 3017, doi: [10.1093/mnras/stt943](https://doi.org/10.1093/mnras/stt943)
- La Barbera, F., Vazdekis, A., Ferreras, I., et al. 2019, *MNRAS*, 489, 4090, doi: [10.1093/mnras/stz2192](https://doi.org/10.1093/mnras/stz2192)
- Labbé, I., van Dokkum, P., Nelson, E., et al. 2023, *Nature*, 616, 266, doi: [10.1038/s41586-023-05786-2](https://doi.org/10.1038/s41586-023-05786-2)
- Larson, R. B. 1998, *MNRAS*, 301, 569

- Leja, J., van Dokkum, P., & Franx, M. 2013, *ApJ*, 766, 33, doi: [10.1088/0004-637X/766/1/33](https://doi.org/10.1088/0004-637X/766/1/33)
- Li, H., Ge, J., Mao, S., et al. 2017, *ApJ*, 838, 77, doi: [10.3847/1538-4357/aa662a](https://doi.org/10.3847/1538-4357/aa662a)
- Lu, J. R., Do, T., Ghez, A. M., et al. 2013, *ApJ*, 764, 155, doi: [10.1088/0004-637X/764/2/155](https://doi.org/10.1088/0004-637X/764/2/155)
- Maraston, C. 1998, *MNRAS*, 300, 872
- Martín-Navarro, I., Barbera, F. L., Vazdekis, A., Falcón-Barroso, J., & Ferreras, I. 2015, *MNRAS*, 447, 1033, doi: [10.1093/mnras/stu2480](https://doi.org/10.1093/mnras/stu2480)
- Mendel, J. T., Beifiori, A., Saglia, R. P., et al. 2020, *ApJ*, 899, 87, doi: [10.3847/1538-4357/ab9ffc](https://doi.org/10.3847/1538-4357/ab9ffc)
- Mercier, W., Shuntov, M., Gavazzi, R., et al. 2024, arXiv e-prints, arXiv:2309.15986, doi: [10.48550/arXiv.2309.15986](https://doi.org/10.48550/arXiv.2309.15986)
- Naidu, R. P., Oesch, P. A., van Dokkum, P., et al. 2022, *ApJL*, 940, L14, doi: [10.3847/2041-8213/ac9b22](https://doi.org/10.3847/2041-8213/ac9b22)
- Nam, D. G., Federrath, C., & Krumholz, M. R. 2021, *MNRAS*, 503, 1138, doi: [10.1093/mnras/stab505](https://doi.org/10.1093/mnras/stab505)
- Newman, A. B., Belli, S., Ellis, R. S., & Patel, S. G. 2018, *ApJ*, 862, 126, doi: [10.3847/1538-4357/aacd4f](https://doi.org/10.3847/1538-4357/aacd4f)
- Offner, S. S. R., Clark, P. C., Hennebelle, P., et al. 2014, in *Protostars and Planets VI*, ed. H. Beuther, R. S. Klessen, C. P. Dullemond, & T. Henning, 53–75, doi: [10.2458/azu_uapress_9780816531240-ch003](https://doi.org/10.2458/azu_uapress_9780816531240-ch003)
- Peacock, M. B., Zepf, S. E., Kundu, A., et al. 2017, *ApJ*, 841, 28, doi: [10.3847/1538-4357/aa70eb](https://doi.org/10.3847/1538-4357/aa70eb)
- Posacki, S., Cappellari, M., Treu, T., Pellegrini, S., & Ciotti, L. 2015, *MNRAS*, 446, 493, doi: [10.1093/mnras/stu2098](https://doi.org/10.1093/mnras/stu2098)
- Salpeter, E. E. 1955, *ApJ*, 121, 161
- Schaerer, D., Guibert, J., Marques-Chaves, R., & Martins, F. 2024, arXiv e-prints, arXiv:2407.12122, doi: [10.48550/arXiv.2407.12122](https://doi.org/10.48550/arXiv.2407.12122)
- Schneider, F. R. N., Sana, H., Evans, C. J., et al. 2018, *Science*, 359, 69, doi: [10.1126/science.aan0106](https://doi.org/10.1126/science.aan0106)
- Shetty, S., Cappellari, M., McDermid, R. M., et al. 2020, *MNRAS*, 494, 5619, doi: [10.1093/mnras/staa1043](https://doi.org/10.1093/mnras/staa1043)
- Smith, R. J. 2020, *ARA&A*, 58, 577, doi: [10.1146/annurev-astro-032620-020217](https://doi.org/10.1146/annurev-astro-032620-020217)
- Spiniello, C., Trager, S. C., Koopmans, L. V. E., & Chen, Y. 2012, ArXiv e-prints. <https://arxiv.org/abs/1204.3823>
- Steinhardt, C. L., Kokorev, V., Rusakov, V., Garcia, E., & Sneppen, A. 2023, *ApJL*, 951, L40, doi: [10.3847/2041-8213/acdef6](https://doi.org/10.3847/2041-8213/acdef6)
- Tanvir, T. S., & Krumholz, M. R. 2024, *MNRAS*, 527, 7306, doi: [10.1093/mnras/stad3581](https://doi.org/10.1093/mnras/stad3581)
- Tanvir, T. S., Krumholz, M. R., & Federrath, C. 2022, *MNRAS*, 516, 5712, doi: [10.1093/mnras/stac2642](https://doi.org/10.1093/mnras/stac2642)
- Tinsley, B. M. 1980, *Fundamentals of Cosmic Physics*, 5, 287
- Torrey, P., Wellons, S., Ma, C.-P., Hopkins, P. F., & Vogelsberger, M. 2017, *MNRAS*, 467, 4872, doi: [10.1093/mnras/stx370](https://doi.org/10.1093/mnras/stx370)
- Treu, T., Auger, M. W., Koopmans, L. V. E., et al. 2010, *ApJ*, 709, 1195, doi: [10.1088/0004-637X/709/2/1195](https://doi.org/10.1088/0004-637X/709/2/1195)
- van de Sande, J., Kriek, M., Franx, M., Bezanson, R., & van Dokkum, P. G. 2015, *ApJ*, 799, 125, doi: [10.1088/0004-637X/799/2/125](https://doi.org/10.1088/0004-637X/799/2/125)
- van de Sande, J., Kriek, M., Franx, M., et al. 2013, *ApJ*, 771, 85, doi: [10.1088/0004-637X/771/2/85](https://doi.org/10.1088/0004-637X/771/2/85)
- van der Wel, A., Rix, H.-W., Wuyts, S., et al. 2011, *ApJ*, 730, 38, doi: [10.1088/0004-637X/730/1/38](https://doi.org/10.1088/0004-637X/730/1/38)
- van Dokkum, P., Brammer, G., Wang, B., Leja, J., & Conroy, C. 2024, *Nature Astronomy*, 8, 119, doi: [10.1038/s41550-023-02103-9](https://doi.org/10.1038/s41550-023-02103-9)
- van Dokkum, P., & Conroy, C. 2021, *ApJ*, 923, 43, doi: [10.3847/1538-4357/ac2a30](https://doi.org/10.3847/1538-4357/ac2a30)
- van Dokkum, P., Conroy, C., Villaume, A., Brodie, J., & Romanowsky, A. J. 2017, *ApJ*, 841, 68, doi: [10.3847/1538-4357/aa7135](https://doi.org/10.3847/1538-4357/aa7135)
- van Dokkum, P. G., & Conroy, C. 2010, *Nature*, 468, 940, doi: [10.1038/nature09578](https://doi.org/10.1038/nature09578)
- van Dokkum, P. G., & Franx, M. 2001, *ApJ*, 553, 90, http://adsabs.harvard.edu/cgi-bin/nph-bib_query?bibcode=2001ApJ...553...90V&db_key=AST
- van Dokkum, P. G., Nelson, E. J., Franx, M., et al. 2015, *ApJ*, 813, 23, doi: [10.1088/0004-637X/813/1/23](https://doi.org/10.1088/0004-637X/813/1/23)
- Wang, B., Leja, J., Atek, H., et al. 2024a, *ApJ*, 963, 74, doi: [10.3847/1538-4357/ad187c](https://doi.org/10.3847/1538-4357/ad187c)
- Wang, B., Leja, J., de Graaff, A., et al. 2024b, arXiv e-prints, arXiv:2405.01473, doi: [10.48550/arXiv.2405.01473](https://doi.org/10.48550/arXiv.2405.01473)
- Woodrum, C., Rieke, M., Ji, Z., et al. 2023, arXiv e-prints, arXiv:2310.18464, doi: [10.48550/arXiv.2310.18464](https://doi.org/10.48550/arXiv.2310.18464)
- Xiao, M., Oesch, P., Elbaz, D., et al. 2023, arXiv e-prints, arXiv:2309.02492, doi: [10.48550/arXiv.2309.02492](https://doi.org/10.48550/arXiv.2309.02492)
- Yan, Z., Jerabkova, T., Kroupa, P., & Vazdekis, A. 2019, *A&A*, 629, A93, doi: [10.1051/0004-6361/201936029](https://doi.org/10.1051/0004-6361/201936029)
- Yan, Z., Jeřábková, T., & Kroupa, P. 2021, *A&A*, 655, A19, doi: [10.1051/0004-6361/202140683](https://doi.org/10.1051/0004-6361/202140683)
- Yung, L. Y. A., Somerville, R. S., Finkelstein, S. L., Wilkins, S. M., & Gardner, J. P. 2024, *MNRAS*, 527, 5929, doi: [10.1093/mnras/stad3484](https://doi.org/10.1093/mnras/stad3484)